Gümüşhane University Journal of Science and Technology

GUFBD / *GUJS* (2026) 16(1): 50-70 doi: 10.17714/gumusfenbil.1791390 Research Article

Some new Schiff base derived thiosemicarbazones: Synthesis, spectroscopic characterization, and theoretical studies

Bazı yeni Schiff bazı türevli tiyosemikarbazonlar: Sentez, spektroskopik karakterizasyon ve teorik çalışmalar

Hasan YAKAN*[1], M. Serdar ÇAVUŞ[2], Halit MUĞLU[3]

[1]*Ondokuz Mayis University, Faculty of Education, Department of Chemistry Education, 55139, Samsun, Türkiye*

[2]*Kastamonu University, Faculty of Engineering and Architecture, Biomedical Engineering Department, 37150, Kastamonu, Türkiye*

[3]*Kastamonu University, Faculty of Science, Department of Chemistry, 37150, Kastamonu, Türkiye*

• Received: 25.09.2025 • Accepted: 11.01.2026

Abstract

A series of some new Schiff base-derived thiosemicarbazones (**1–6**) were synthesized from various aldehydes and *N*-(*o*-tolyl)hydrazinecarbothioamide. The thiosemicarbazide was prepared by the reaction of 1-isothiocyanato-2-methylbenzene with hydrazine monohydrate. The structures and purity of these compounds were confirmed using standard spectroscopic methods, including proton and carbon nuclear magnetic resonance (^{1}H and ^{13}C NMR), Fourier-transform infrared spectroscopy (FT-IR), and elemental analysis. The structural and electronic properties of the compounds were examined using Density Functional Theory (DFT) calculations, and their relationship to structural characterization was analysed and discussed. Additionally, the influence of substituent groups on both the electronic properties and activation behaviors of the compounds was explored.

Keywords: DFT calculations, Schiff base, Structure elucidation, Thiosemicarbazones

Öz

*Çeşitli aldehitler ve N-(o-tolil)hidrazinkarbotiyoamidden bir dizi yeni Schiff bazı türevi tiyosemikarbazonlar (**1-6**) sentezlendi. Tiyosemikarbazit, 1-izotiyosiyanato-2-metilbenzenin hidrazin monohidrat ile reaksiyonuyla hazırlandı. Yeni sentezlenen tüm bileşiklerin yapıları ve saflığı, proton ve karbon nükleer manyetik rezonans (^{1}H ve ^{13}C NMR), Fourier dönüşümlü kızılötesi spektroskopisi (FT-IR) ve element analizi dahil olmak üzere standart spektroskopik yöntemler kullanılarak doğrulandı. Bileşiklerin yapısal ve elektronik özellikleri Yoğunluk Fonksiyonel Teorisi (DFT) hesaplamaları kullanılarak incelendi ve yapısal karakterizasyonla ilişkileri analiz edildi ve tartışıldı. Ayrıca, sübstitüent grupların bileşiklerin hem elektronik özellikleri hem de aktivasyon davranışları üzerindeki etkisi araştırıldı.*

Anahtar kelimeler: *DFT hesaplamaları, Schiff bazı, Yapı aydınlatılması, Tiyosemikarbazonlar*

1. Introduction

Thiosemicarbazones represent an important class of compounds in synthetic organic chemistry, distinguished by their organosulfur framework containing the –NH–C(=S)NH–N= functional group. Due to their structural versatility, they serve as valuable intermediates in the synthesis of a wide range of biologically active molecules. These compounds have been extensively explored for their diverse pharmacological and biological activities, including antitubercular (Netalkar et al., 2014), antiviral (Sevinçli et al., 2020), antimicrobial (Gündüz et al., 2021), antibacterial (Govender et al., 2019), anticonvulsant (Kshirsagar et al., 2009), urease inhibitor (Pervez et al., 2010), anticancer (Shakya & Yadav, 2020), and antioxidant (Muğlu et al., 2022; Hernández et al., 2023; Çavuş, 2025) properties. Nowadays, Schiff base-derived thiosemicarbazones have attracted significant attention for their potential in both in vitro and in vivo biological evaluations. These derivatives have demonstrated notable anticancer (Arafath, 2024), antioxidant (Muğlu, 2020), antibacterial and antifungal (Pervez et al., 2008), antimicrobial (Al-Amiery et al., 2012), enzyme inhibitory properties (Tokalı

*Hasan YAKAN; hasany@omu.edu.tr

et al., 2021), anti-HIV (Bal et al., 2005), ameliorative effect (Karakuş et al., 2024), and anti-inflammatory (Subhashree et al., 2017) activities.

In this research, some new Schiff base derived thiosemicarbazones (**1-6**) were synthesized and thoroughly characterized using FT-IR, ^{1}H-NMR, ^{13}C-NMR spectroscopy, and elemental analysis. Additionally, DFT calculations were employed to gain insights into both the geometric and electronic structures of the synthesized compounds. Through these theoretical analyses, the effects of substituent groups incorporated into the compound structure on the electronic parameters, such as frontier molecular orbital (FMO) energies and global reactivity, and thus their influence on the stability and activity of the compounds, were investigated.

2. Materials and methods

2.1. Materials

Reagents were acquired from commercial suppliers (Merck, Sigma, or Aldrich) and used directly without purification. Spectroscopic grade solvents were used throughout the study. Elemental analyses were carried out using a Eurovector EA3000-Single analyzer. Melting points were measured using a Stuart SMP30 apparatus. FT-IR analysis was performed on a Bruker Alpha spectrometer. Proton and carbon NMR spectra (^{1}H and ^{13}C) were recorded on a Bruker Avance DPX-400 MHz using DMSO-d_6 as solvent.

2.2. Synthesis of the compounds (1-6)

A mixture of 1-isothiocyanato-2-methylbenzene (7.50 mmol) and hydrazine monohydrate (7.50 mmol) was added dropwise to 20 mL of ethanol under vigorous stirring, while maintaining the temperature in an ice bath. The mixture was placed in a refrigerator and left to stand overnight. The resulting precipitate, corresponding to the thiosemicarbazide, was filtered, dried, and purified using ethanol. Afterwards, a few drops of hydrochloric acid were added to a solution containing the thiosemicarbazide (4.00 mmol) and various aldehydes (4.00 mmol) in 20 mL of aqueous ethanol. The reaction mixture was refluxed at 78 °C for 3 to 5 hours. Upon completion, the solid product was collected by filtration, washed, and air-dried. The target Schiff base-derived thiosemicarbazones were successfully synthesized in good yields (66-88%) as shown in Figure 1. A previously reported method was followed with slight modifications (Zhang et al., 2007; Yakan, 2020).

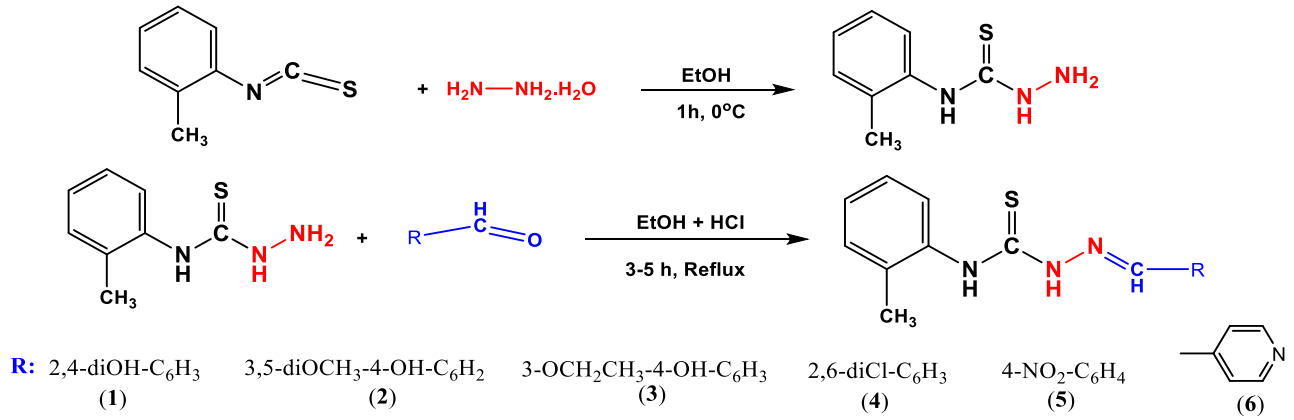

Figure 1. Synthesis pathway of new Schiff base derived thiosemicarbazones (**1-6**).

2.3. Theoretical studies

All quantum chemical calculations were performed based on DFT (Hohenberg & Kohn, 1964; Kohn & Sham, 1965) using the ORCA software (Neese, 2022). The B3LYP functional (Becke, 1988; Lee et al., 1988), combined with the D4 dispersion correction (Caldeweyher et al., 2017; Caldeweyher et al., 2020) and the 6-311++G(2d,2p) basis set (Lee et al., 1988; McLean & Chandler, 1980), was employed. No symmetry constraints were applied during the optimization of molecular structures. To achieve more precise convergence, the TightSCF and TightOpt algorithms were activated, and automatic auxiliary basis sets were generated using the AutoAux command. Analysis of the IR spectra confirmed that the structures exhibited no negative vibrational modes.

Gas-phase calculations were utilized to elucidate the electronic structures and reactivity properties of the molecules. These data were evaluated through Highest Occupied Molecular Orbital (HOMO) and Lowest Unoccupied Molecular Orbital (LUMO) energy levels and used to calculate global reactivity descriptors (such as electrophilic index (ω), electronegativity (χ), chemical hardness (η), nucleophilic index (ε), etc.).

The electronic chemical potential (μ) is fundamentally defined as the first derivative of the total energy (E) with respect to the number of electrons (N) at a constant external potential v(r) (Parr, 1980; Parr & Pearson, 1983):

$$\mu = \left(\frac{\partial E}{\partial N}\right)_{v(r)} \quad (1)$$

Within the framework of DFT, applying the finite difference approximation and Koopmans' theorem (Koopmans, 1934; Kohn & Sham, 1965) the electronic chemical potential (μ) was approximated as:

$$\mu \approx \frac{(E_{HOMO}+E_{LUMO})}{2} \quad (2)$$

Subsequently, electronegativity (χ) (Parr et al., 1999) and chemical hardness (η) (Pearson, 1988) were defined by the equations:

$$\chi = -\mu \quad (3)$$

$$\eta = \frac{(E_{LUMO}-E_{HOMO})}{2} \quad (4)$$

The electrophilicity index ω is given by the expression (Parr et al., 1999):

$$\omega = \frac{\mu^2}{2\eta} \quad (5)$$

The relative empirical nucleophilic index, ε, is defined using tetracyanoethylene (TCE) as a reference (Domingo et al., 2008):

$$\varepsilon = E_{HOMO(Nucleophile)} - E_{HOMO(TCE)} \quad (6)$$

Finally, the electroaccepting, ω^+, and electrodonating, ω^-, powers were calculated as follows (Gázquez et al., 2007):

$$\omega^+ = \frac{A^2}{2(I-A)} \quad (7)$$

$$\omega^- = \frac{I^2}{2(I-A)} \quad (8)$$

where ω^+ quantifies the ability to accept electron density, while ω^- quantifies the ability to donate it.

Additionally, for NMR calculations, the solvent environment was accounted for using the CPCM-SCRF model (Cossi et al., 1996), with re-optimizations performed in DMSO. NMR calculations at the B3LYP/6-311++G(2d,2p) level determined chemical shifts by subtracting the absolute magnetic shielding values of the reference compound TMS (31.805 ppm for ^{1}H; 183.726 ppm for ^{13}C).

3. Results and discussion

3.1. Physicochemical data

The physicochemical and analytical data are compiled in Tables 1 and 2.

Table 1. The physicochemical data of the compounds.

Comp.	Compounds' Structure	M. P. (°C)	Yields (%)	Colour
1	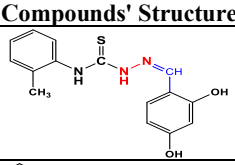	122-123	73	Dark Brown
2	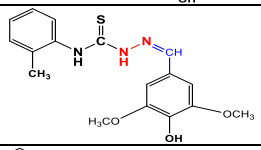	192-193	79	White
3	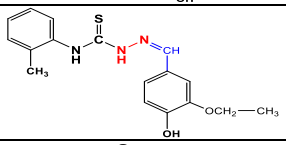	194-195	88	White
4	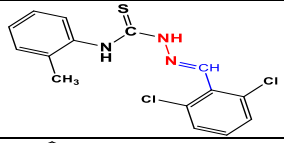	198-199	77	White
5	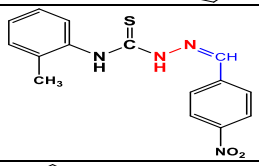	212-213	70	Yellow
6	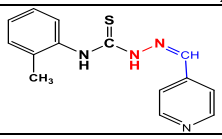	187-188	66	White

Table 2. Elemental analysis results of the compounds

			Calculated			Experimental		
Comp.	**Mol. Formula**	**M.W. (g/mol)**	**C%**	**H%**	**N%**	**C%**	**H%**	**N%**
1	$C_{15}H_{15}N_3O_2S$	301.36	59.78	5.02	13.94	59.73	5.03	13.96
2	$C_{17}H_{19}N_3O_3S$	345.42	59.11	5.54	12.17	59.15	5.53	12.16
3	$C_{17}H_{19}N_3O_2S$	329.42	61.98	5.81	12.76	62.04	5.80	12.78
4	$C_{15}H_{13}Cl_2N_3S$	338.25	53.26	3.87	12.42	53.23	3.88	12.45
5	$C_{15}H_{14}N_4O_2S$	314.36	57.31	4.49	17.82	57.28	4.49	17.85
6	$C_{14}H_{14}N_4S$	270.35	62.20	5.22	20.72	62.27	5.21	20.68

3.2. IR spectral analysis

Considering the FT-IR spectra of the compounds, the asymmetric and symmetric stretching frequencies of the amino group (–NH_2) as a characteristic doublet peak were not observed at 3400 – 3200 cm^{-1}. At the same time, aldehyde frequencies (–CHO, two bands) of aldehydic region were not shown at 2820 – 2700 cm^{-1}. Instead, a novel imine group (CH=N) vibration was observed at 1588 – 1532 cm^{-1}. This evidence confirmed the expected successful reaction. For all compounds (**1-6**), a novel amine group (-NH) vibration were detected in the range 3326 - 3090 cm^{-1}, aromatic and aliphatic protons were observed at 3078 – 2957 cm^{-1} and 2942 – 2863 cm^{-1}. The –C=S signals were observed at 1426 – 1315 cm^{-1}, the –C–N vibrations were observed at 1287 – 1174 cm^{-1} (see Figures S1-S6 in Supplementary information). For the compounds **1**–**3**, the –C–O vibrations were observed at 1167 and 1039 cm^{-1}, the –OH vibrations were observed in the range of 3495 – 3423 cm^{-1}. For the compound **4**, the –C–Cl vibration signal was observed at 1079 cm^{-1}. For compound **5**, the nitro (–NO_2) group were observed at 1496 and 1177 cm^{-1}. These findings align with earlier data reported for structurally similar compounds (Al-Amiery et al., 2012; Yakan, Azam, et al., 2023; Yakan, Muğlu, et al., 2023; Sarıoğlu & Soğukömeroğulları, 2024). These findings confirm the successful outcome of the expected reaction. The principal IR stretching bands detected in the synthesized compounds are summarized in Table 3.

Table 3. Experimental and calculated IR vibration frequencies of the synthesized compounds (cm^{-1}).

	Comp.	υ_{NH}	υ_{C-H} (Aromatic)	υ_{C-H} (Aliphatic)	$\upsilon_{C=N}$	$\upsilon_{C=S}$	υ_{C-N}	υ_{C-O}	Specific Vib.
Experimental	**1**	3162	3025	2876	1536	1323	1219 1174	1122 1106	OH: 3423
	2	3246 3148	3032-2998	2907-2876	1546	1315	1208 1185	1107 1039	OH: 3497
	3	3269 3189	3067-2988	2942-2879	1532	1370	1266 1243	1167 1114	OH: 3495
	4	3326 3117	3012-2964	2914-2882	1534	1426	1287 1259	-	C-Cl: 1079
	5	3299 3090	2957	2863	1582	1338	1283 1257	-	NO_2: 1496, 1177
	6	3298 3112	3078-3022	2925	1588	1384	1259 1222	-	-
Calculated	**1**	3605.27 3543.67	3235.01- 3113.48	3065.86	1645.32	1423.20	1278.85 1227.67	1211.30 1149.16	OH: 3827.65 OH: 3473.77
	2	3541.01 3532.83	3236.26- 3083.88	3058.06	1661.12	1433.14	1276.79 1225.62	1122.43 1057.65	OH: 3767.09
	3	3540.05 3533.03	3235.51- 3162.96	3114.63- 3007.65	1663.77	1439.15	1277.84 1225.45	1273.70 1199.83	OH: 3769.32
	4	3530.93 3517.52	3230.35- 3112.00	3107.23- 3023.54	1653.50	1460.47	1277.45 1219.87	-	C-Cl: 1094.06
	5	3546.72 3519.65	3239.16- 3114.98	3065.01- 3009.63	1656.02	1434.57	1271.25 1217.63	-	NO_2: 1558.76, 1359.32
	6	3543.56 3522.78	3238.48- 3113.34	3062.50- 3010.29	1655.70	1433.82	1267.48 1218.71	-	-

3.3. ^{1}H NMR analysis

The ^{1}H NMR spectra of the compounds were acquired in DMSO-d_6 and the results are presented in Table 4. For all compounds **1-6**, the amino signal (-NH, H7) of thiosemicarbazone moiety was observed as a singlet in the ranges of 12.16 – 11.48 ppm, while the amino signal (–NH, H6) of 2-methylphenyl region was resonated as a singlet at 10.23 – 8.89 ppm, respectively. The characteristic proton signal of imine (–CH=N, H8) was detected as a singlet in the ranges of 8.42 – 8.03 ppm. The methyl proton (–CH_3, H5) signals of 2-methylphenyl region were observed as a singlet at between 2.26 and 2.21 ppm. The aromatic proton (H1-H4) signals of 2-methylphenyl region were resonated in the ranges of 8.26 – 7.20 ppm. The aromatic proton (H9-H13) signals of aldehyde region were detected in the ranges of 8.62 – 6.26 ppm (see Figures S7-S12 in Supplementary information).

The each –OH proton signals of compounds **1-3** were observed as a singlet at 9.78 (2H), 9.84, and 9.83 ppm, respectively. The methoxy proton signal of compound **2** was observed as a singlet at 3.82 ppm. For compounds **3**, the proton signal of the methylene group (OCH_2) was observed as a quartet at 4.11 – 4.06 ppm (q, 2H); the –CH_3 proton signal was detected as a triplet at 1.36 – 1.33 ppm (t, 2H). The obtained data are in accordance with previously reported results for similar compounds (Al-Amiery et al., 2012; Yakan, Azam, et al., 2023; Yakan, Muğlu, et al., 2023; Sarıoğlu & Soğukömeroğulları, 2024). The DMSO-d_6 signal appeared as a quintet at approximately 2.50 ppm, while the water signal (HOD or H_2O in DMSO) was observed around 3.30 ppm, with its exact position varying depending on solvent composition and concentration (Fleming & Williams, 2020).

3.4. ^{13}C NMR interpretations

The ^{13}C NMR spectra of the synthesized compounds were detected in DMSO-d_6 and the chemical shifts are presented in Table 5. For compounds **1**–**6**, the characteristic –C=S peaks were detected at 177.81 – 176.41 ppm. The other characteristic –CH=N (imine) peaks were observed in the ranges 143.71 – 138.16 ppm. The methyl carbon (–CH_3) signals of 2-methylphenyl region were observed at between 18.32 and 18.04 ppm. The aromatic carbon atom (C1-C6) signals of 2-methylphenyl region were detected in the ranges of 138.69 – 126.28 ppm. The aromatic carbon atom (C7-C12) signals of aldehyde region were observed in the ranges of 161.06 – 102.74 ppm (see Figures S13-S18 in Supplementary information).

Table 4. Experimental and calculated ^{1}H NMR data of the compounds, (δ/ppm).

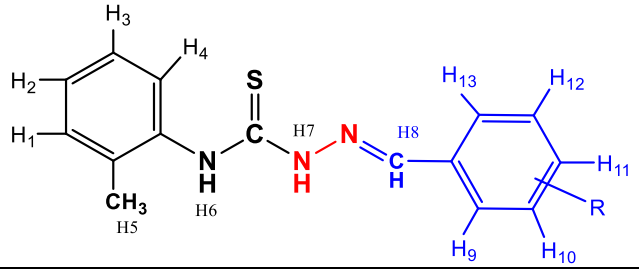

	Comp.	H1-H4	H5*, CH_3	H6˙, NH	H7˙, NH	H8˙, CH=N	H9-H13	Specific Peak
Experimental	1	7.42-7.20 (m)	2.23	9.78	11.48	8.35	7.84 (s), 6.41-6.26 (m)	OH: 9.78 (s, 2H)
	2	7.38-7.36 (d), 7.30-7.28 (dd), 7.25-7.21 (ddd)	2.26	8.89	11.73	8.04	7.13 (s),	OH: 9.84 (s) OCH_3: 3.82 (s)
	3	7.37-7.35 (d), 7.30-7.21 (dt)	2.25	9.44	11.64	8.03	7.54 (s), 7.13-7.11 (d), 6.83-6.81 (d),	OH: 9.83 (s), OCH_2: 4.11-4.06 (q), CH_3: 1.36-1.33 (t)
	4	7.59-7.57 (d), 7.49-7.42 (m)	2.21	9.57	12.16	8.42	7.26-7.16 (m)	-
	5	8.26-8.19 (m)	2.24	10.23	12.10	8.23	7.31-7.23 (m)	-
	6	7.31-7.23 (m)	2.24	10.19	12.08	8.11	8.62-8.61 (d), 7.90-7.88 (d)	-
Calculated	1	7.68-7.84	2.22-2.64	8.28	9.02	8.33	6.78-6.91	OH: 10.84, 5.74 OH: 6.32
	2	7.70-8.13	2.36-2.72	9.38	9.12	8.10	7.92, 7.24	OCH_3: 3.71-4.25, 4.03-4.39
	3	7.75-7.94	2.33-2.71	9.20	9.11	8.13	7.35-8.03	OH: 6.48, OCH_2: 4.32, 4.33, CH_3: 1.48-1.63
	4	7.77-7.88	2.25-2.56	9.38	9.46	8.68	7.75-7.91	-
	5	7.57-10.19	2.73-2.94	10.67	9.31	8.28	8.03-8.9	-
	6	7.57-10.24	2.71-2.93	10.60	9.25	8.15	7.80-9.16	-

* (s, 3H) ˙(s, 1H)

For all compounds, some carbon atom signals (161.06 – 129.00 ppm) were shifted down-field (high values of δ) relative to the signal of phenyl carbon (128.5 ppm) due to the presence of methoxy (–OCH_3), –OH, nitrogen, methyl (–CH_3), –Cl, –NO_2 atoms/groups. The methoxy (–OCH_3) carbon signal of compound **2** was observed at 56.68 ppm. For compounds **3**, the carbon signal of the methylene group (OCH_2) was observed at 64.47 ppm; the methyl (–CH_3) carbon signal of ethyl group was detected at 15.16 ppm. These values align well with those documented for similar molecular structures in prior studies (Al-Amiery et al., 2012; Hussein et al., 2019; Yakan, Azam, et al., 2023; Yakan, Muğlu, et al., 2023; Rizvi et al., 2024).

3.5. DFT analysis

As detailed in Figure 2, it was observed in this study that the HOMO and LUMO distributions of all six compounds examined are distinctly separated in different regions of the molecule. HOMO localization is concentrated around the aldehyde moiety in compounds **1**–**3**, around the 2-methylphenyl site in compounds **4**–**6**, and commonly around sulfur and adjacent nitrogen atoms. ESP maps indicate that the electron density is concentrated around atoms such as the sulphur atom, the oxygens in the nitro group (compound **5**), and the phenolic/etheric oxygens (compounds **1**–**3**). This localization suggests that this site of the molecule exhibits nucleophilic character and is the most susceptible region to electrophilic attacks. In contrast, LUMO localization is observed on the thiourea-aldehyde region, with a notable decrease in electron density around the hydrogen atoms of the amine (N-H) and hydroxyl (O-H) groups. These findings indicate that this region is electrophilic and the most reactive toward nucleophilic attacks.

Table 5. Experimental and calculated ^{13}C NMR data of the compounds, (δ/ppm).

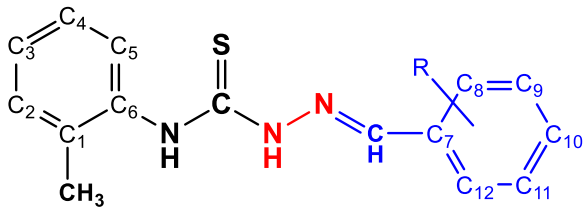

		1	2	3	4	5	6
Experimental	**CH_3**	18.31	18.32	18.30	18.04	18.25	18.24
	C=S	176.41	176.70	176.68	177.30	177.76	177.81
	CH=N	141.13	138.38	143.71	138.16	141.20	141.91
	C1	135.63	135.87	135.82	134.53	136.16	136.11
	C2	130.47	130.55	130.52	130.58	130.59	130.58
	C3	129.00	129.14	129.11	129.76	129.33	129.31
	C4	126.28	126.38	125.95	126.31	126.50	126.47
	C5	126.90	127.10	127.04	126.90	127.43	127.40
	C6	138.69	138.67	138.67	137.84	138.45	138.43
	C7	112.31	124.73	126.35	131.63	140.19	140.05
	C8	161.06	105.65	111.27	134.57	128.85	121.79
	C9	102.74	148.59	147.72	128.09	124.23	150.49
	C10	158.57	143.76	149.69	130.30	148.08	-
	C11	108.23	148.59	115.80	128.09	124.23	150.49
	C12	133.44	105.65	123.16	134.57	128.85	121.79
	R	-	OCH_3: 56.68	OCH_2: 64.47 CH_3: 15.16	-	-	-
Calculated	**CH_3**	20.06	19.96	20.06	20.01	19.78	19.76
	C=S	183.59	183.68	184.21	186.21	180.67	180.75
	CH=N	153.81	149.54	149.86	143.39	144.95	145.34
	C1	147.40	142.10	143.64	144.40	135.50	135.50
	C2	136.38	135.77	135.84	136.00	136.30	136.40
	C3	134.98	132.42	133.19	133.90	129.90	129.50
	C4	132.30	130.70	131.06	131.40	131.80	131.60
	C5	135.33	134.30	135.65	136.00	121.20	121.00
	C6	144.91	144.00	144.44	144.30	144.50	144.60
	C7	116.08	131.50	132.22	135.80	149.70	148.70
	C8	168.42	126.10	109.71	151.10	137.30	130.50
	C9	105.94	153.90	153.99	134.90	131.90	159.00
	C10	169.00	150.60	156.81	136.40	154.30	-
	C11	111.82	155.60	118.07	136.60	131.20	157.70
	C12	141.16	105.50	131.30	147.10	130.10	122.80
	R	-	OCH_3: 58.34, 64.31	OCH_2: 69.32 CH_3: 15.53	-	-	-

The incorporation of electron-donating groups (EDGs) into the aryl ring generates an effect that enhances molecular stability. In compounds **1**, **2**, and **3**, these groups donate electron density to the π-system through resonance and inductive effects, destabilizing both HOMO and LUMO energy levels, which leads to a widening of the HOMO-LUMO energy gap (E_g). These compounds exhibit the widest energy gaps in the series, ranging from 3.809 eV to 3.824 eV (Table 6). A wide energy gap indicates high resistance to electronic excitations and, consequently, high kinetic stability. Therefore, derivatives containing EDGs stand out as chemically less reactive but more stable structures. Among these groups, the ethoxy-substituted compound **3**, with the highest HOMO energy (-5.707 eV), is considered the most effective electron donor. Conversely, the presence of electron-withdrawing groups (EWGs) such as chloro (-Cl), nitro ($-NO_2$), and 4-pyridinyl significantly enhances molecular reactivity. These groups withdraw electron density from the aryl ring, lowering the energy of the LUMO orbital, which acts as an electron acceptor.

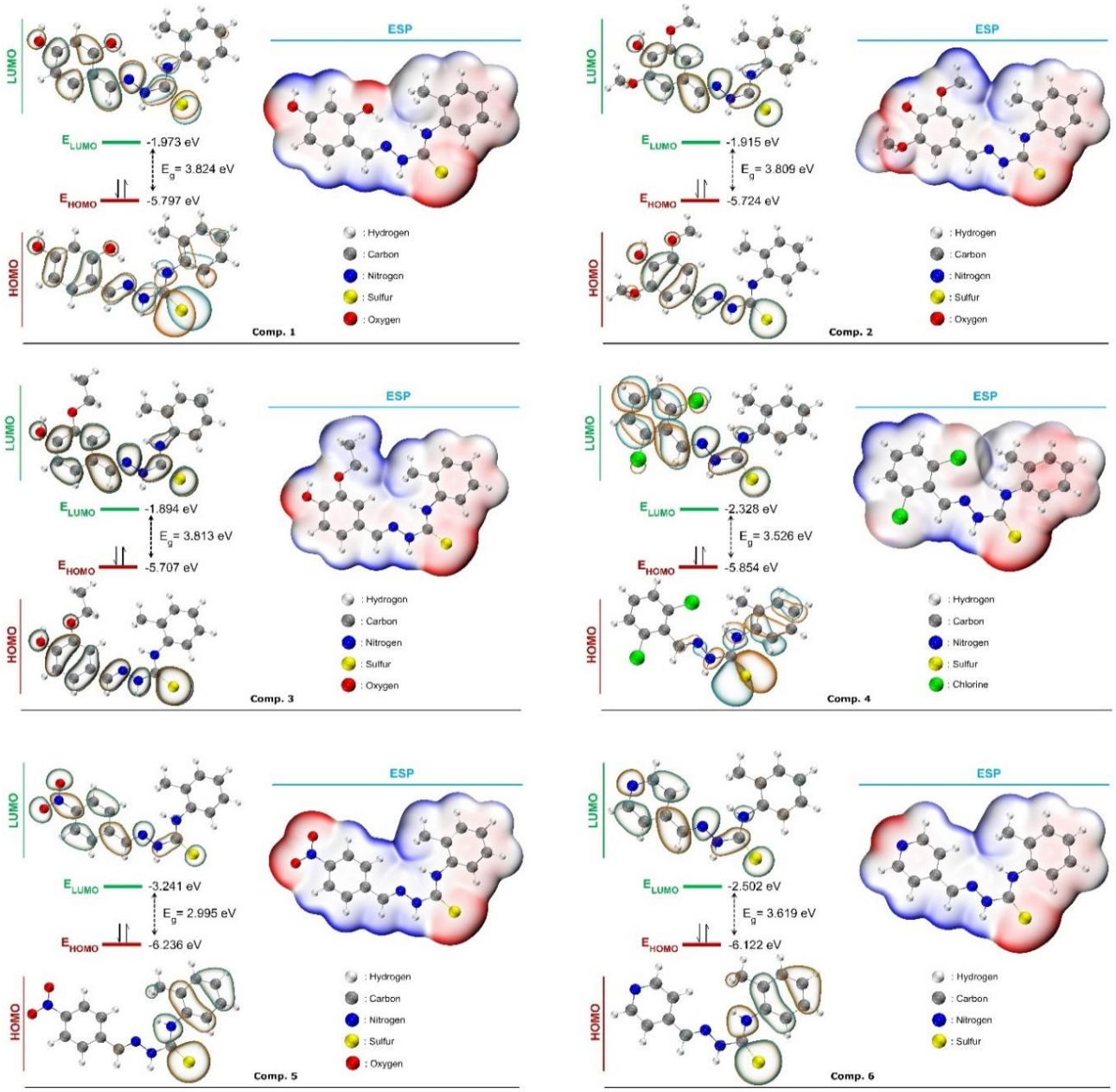

Figure 2. HOMO-LUMO and ESP surface of the compounds.

A lower-energy LUMO makes the molecule a better electron acceptor, and the narrowing of the energy gap renders these compounds more prone to chemical reactions. This effect is most pronounced in compound **5**, which contains the strongly electron-withdrawing *p*-nitro group. The E_g value of this compound, 2.995 eV, is lower than that of the other compounds, making compound **5** stand out as the most reactive among all. The data indicate that the electron-withdrawing strength follows the order $–NO_2$ (**5**) > –Cl (**4**) > 4-pyridinyl (**6**). Global reactivity parameters also support these findings. While the most stable compound, compound **1**, exhibits the highest hardness (η = 1.912 eV), the most reactive compound, compound **5**, has the lowest hardness value (η = 1.498 eV). These data reveal a kinetic stability order of **1** > **3** > **2** > **6** > **4** > **5**.

Moreover, compound **5** exhibits the highest electrophilicity index (ω) in the series at 7.496 eV, making it the strongest electrophile. This finding is consistent with compound **5** having the lowest LUMO energy (-3.241 eV) and the highest electron-accepting power (ω^+ = 1.753 eV). In contrast, compounds with electron-donating groups (**1**, **2**, **3**) are weak electron acceptors, with low ω^+ values around 0.5 eV. Regarding electron-donating capability, compound **3** has been identified as the best electron donor, with the highest HOMO energy (-5.707 eV), the lowest electron-donating power index (ω^- = 4.271 eV), and highest nucleophilicity index (ε = 3.788 eV). On the other hand, compound **5**, characterized by the lowest HOMO energy (-6.236 eV) and the lowest nucleophilicity index (ε = 3.259 eV), is the weakest electron donor.

Table 6. Calculated electronic parameters of the compounds.

Comp.	E_{HOMO} (eV)	E_{LUMO} (eV)	E_g (eV)	η (eV)	χ (eV)	ω (eV)	ε (eV)	ω^+ (eV)	ω^- (eV)
1	-5.797	-1.973	3.824	1.912	3.885	3.947	3.698	0.509	4.394
2	-5.724	-1.915	3.809	1.905	3.820	3.830	3.770	0.481	4.301
3	-5.707	-1.894	3.813	1.907	3.800	3.787	3.788	0.470	4.271
4	-5.854	-2.328	3.526	1.763	4.091	4.746	3.641	0.768	4.859
5	-6.236	-3.241	2.995	1.498	4.738	7.496	3.259	1.753	6.491
6	-6.122	-2.502	3.619	1.810	4.312	5.137	3.373	0.865	5.177

E_g: $E_{LUMO} - E_{HOMO}$, η: Chemical Hardness, χ: Electronegativity, ω: Electrophilic index, ε: Nucleophilic index, ω^+ : Electroaccepting power, ω^- : Electrodonating power

4. Conclusions

A series of novel Schiff base-derived thiosemicarbazones were effectively synthesized and obtained in moderate to good yields ranging from 66% to 88%. The chemical structures of all compounds were confirmed using IR spectroscopy, ^{1}H and ^{13}C NMR spectroscopy, as well as elemental analysis.

In this study, the electronic properties and chemical reactivities of thiosemicarbazone derivatives containing different substituents were systematically investigated using DFT calculations. Global reactivity parameters such as chemical hardness, electrophilicity, electroaccepting/electrodonating power, and nucleophilicity were employed to predict the behavior of the compounds. The obtained results revealed that compounds with electron-donating groups exhibit a wider HOMO-LUMO energy gap, indicating greater kinetic stability and higher resistance to chemical reactions. In contrast, electron-withdrawing groups were observed to lower the LUMO energy, thereby increasing reactivity, with compound **5** (containing the *p*-nitro group) identified as the most reactive structure.

Acknowledgement

This study was not supported by any organization. We would like to thank to TUBITAK ULAKBIM, High Performance and Grid Computing Center (TRUBA resources) for theoretical calculations. The editor and referee/referees should be thanked for their contributions during the review and evaluation of the manuscript.

Author contribution

HY: article administration, writing–review, investigation, visualization & editing. MSÇ: dft calculations, writing - original draft, writing–review. HM: methodology, writing - original draft, writing–review. All authors reviewed the manuscript.

Declaration of ethical code

The authors of this article declare that the materials and methods used in this study do not require ethics committee approval and/or legal-special permission.

Conflicts of interest

The authors declare that there is no conflict of interest.

Supplementary material

All spectra of the compounds are given in the supplementary materials.

References

Al-Amiery, A. A., Al-Majedy, Y. K., Ibrahim, H. H., & Al-Tamimi, A. A. (2012). Antioxidant, antimicrobial, and theoretical studies of the thiosemicarbazone derivative Schiff base 2-(2-imino-1-methylimidazolidin-4-ylidene) hydrazinecarbothioamide (IMHC). *Organic and Medicinal Chemistry Letters*, *2*(4), 1-7.

Arafath, M. A. (2024). Thiosemicarbazone Schiff base ligands and their complexes with nickel, palladium and platinum show anticancer and antibacterial activities. *Journal of Sulfur Chemistry*, *45*(1), 138-171.

Bal, T. R., Anand, B., Yogeeswari, P., & Sriram, D. (2005). Synthesis and evaluation of anti-HIV activity of isatin β-thiosemicarbazone derivatives. *Bioorganic and Medicinal Chemistry Letters*, *15*(20), 4451-4455.

Becke, A. D. (1988). Density-functional exchange-energy approximation with correct asymptotic behavior. *Physical review A*, *38*(6), 3098.

Caldeweyher, E., Bannwarth, C., & Grimme, S. (2017). Extension of the D3 dispersion coefficient model. *The Journal of chemical physics*, *147*(3).

Caldeweyher, E., Mewes, J.-M., Ehlert, S., & Grimme, S. (2020). Extension and evaluation of the D4 London-dispersion model for periodic systems. *Physical Chemistry Chemical Physics*, *22*(16), 8499-8512.

Cossi, M., Barone, V., Cammi, R., & Tomasi, J. (1996). Ab initio study of solvated molecules: a new implementation of the polarizable continuum model. *Chemical Physics Letters*, *255*(4-6), 327-335.

Çavuş, M. S. (2025). Synthesis of new 5-iodoisatin derivatives: Predicting antioxidant inhibition activity with DFT studies. *Journal of Molecular Structure*, *1323*, 140826.

Domingo, L. R., Chamorro, E., & Pérez, P. (2008). Understanding the reactivity of captodative ethylenes in polar cycloaddition reactions. A theoretical study. *Journal of Organic Chemistry*, *73*(12), 4615-4624.

Fleming, I., Williams, D. (2020). 1D Nuclear Magnetic Resonance Spectra. In: Spectroscopic Methods in Organic Chemistry. Springer, Cham., pp. 123-276. https://doi.org/10.1007/978-3-030-18252-6_4

Gázquez, J. L., Cedillo, A., & Vela, A. (2007). Electrodonating and electroaccepting powers. *Journal of Physical Chemistry A*, *111*(10), 1966-1970.

Govender, H., Mocktar, C., Kumalo, H. M., & Koorbanally, N. A. (2019). Synthesis, antibacterial activity and docking studies of substituted quinolone thiosemicarbazones. *Phosphorus, Sulfur, and Silicon and the Related Elements*, *194*(11), 1074-1081.

Gündüz, M. G., Kaya, B., Özkul, C., Şahin, O., Rekha, E. M., Sriram, D., & Ülküseven, B. (2021). S-alkylated thiosemicarbazone derivatives: Synthesis, crystal structure determination, antimicrobial activity evaluation and molecular docking studies. *Journal of Molecular Structure*, *1242*, 130674.

Hernández, W., Carrasco, F., Vaisberg, A., Spodine, E., Icker, M., Krautscheid, H., Beyer, L., Tamariz-Angeles, C., & Olivera-Gonzales, P. (2023). Novel thiosemicarbazone derivatives from furan-2-carbaldehyde: synthesis, characterization, crystal structures, and antibacterial, antifungal, antioxidant, and antitumor activities. *Journal of Chemistry*, *2023*, 1-20.

Hohenberg, P., & Kohn, W. (1964). Inhomogeneous Electron Gas. *Physical Review*, *136*(3B), B864-B871.

Hussein, M. A., Iqbal, M. A., Umar, M. I., Haque, R. A., & Guan, T. S. (2019). Synthesis, structural elucidation and cytotoxicity of new thiosemicarbazone derivatives. *Arabian Journal of Chemistry, 12(8),* 3183-3192.

Karakuş, F. G., Tunalı, S., Bal-demirci, T., Ülküseven, B., & Yanardağ, R. (2024). Ameliorative Effect of a Vanadium-thiosemicarbazone Complex on Oxidative Stress in Stomach Tissue of Experimental Diabetic Rats. *Sakarya University Journal of Science*, *28*(1), 133-144.

Kohn, W., & Sham, L. J. (1965). Self-consistent equations including exchange and correlation effects. *Physical Review*, *140*(4A), A1133-A1138.

Koopmans, T. (1934). Über die Zuordnung von Wellenfunktionen und Eigenwerten zu den einzelnen Elektronen eines Atoms. *physica*, *1*(1-6), 104-113.

Kshirsagar, A., Toraskar, M. P., Kulkarni, V. M., Dhanashire, S., & Kadam, V. (2009). Microwave assisted synthesis of potential anti infective and anticonvulsant thiosemicarbazones. *International Journal of ChemTech Research*, *1*(3), 696-701.

Lee, C., Yang, W., & Parr, R. G. (1988). Development of the Colle-Salvetti correlation-energy formula into a functional of the electron density. *Physical review B*, *37*(2), 785.

McLean, A., & Chandler, G. (1980). Contracted Gaussian basis sets for molecular calculations. I. Second row atoms, Z= 11–18. *Journal of Chemical Physics*, *72*(10), 5639-5648.

Muğlu, H. (2020). Synthesis, characterization, and antioxidant activity of some new N 4-arylsubstituted-5-methoxyisatin-β-thiosemicarbazone derivatives. *Research on Chemical Intermediates, 46(4)*, 2083-2098.

Muğlu, H., Kurt, B. Z., Sönmez, F., Güzel, E., Çavuş, M. S., & Yakan, H. (2022). Preparation, antioxidant activity, and theoretical studies on the relationship between antioxidant and electronic properties of bis (thio/carbohydrazone) derivatives. *Journal of Physics and Chemistry of Solids*, *164*, 110618.

Neese, F. (2022). Software update: The ORCA program system-Version 5.0. *Wiley Interdisciplinary Reviews: Computational Molecular Science*, *12*(5), e1606.

Netalkar, P. P., Netalkar, S. P., & Revankar, V. K. (2014). Nickel (II) complexes of thiosemicarbazones: synthesis, characterization, X-ray crystallographic studies and in vitro antitubercular and antimicrobial studies. *Transition Metal Chemistry*, *39*, 519-526.

Parr, R. G. (1980). Density functional theory of atoms and molecules. Horizons of Quantum Chemistry: Proceedings of the Third International Congress of Quantum Chemistry, October 29-November 3, 1979, Kyoto, Japan.

Parr, R. G., & Pearson, R. G. (1983). Absolute hardness: companion parameter to absolute electronegativity. *Journal of the American Chemical Society*, 105(26), 7512-7516.

Parr, R. G., Szentpály, L. v., & Liu, S. (1999). Electrophilicity index. *Journal of the American Chemical Society*, 121(9), 1922-1924.

Pearson, R. G. (1988). Chemical hardness and bond dissociation energies. *Journal of the American Chemical Society*, 110(23), 7684-7690.

Pervez, H., Iqbal, M. S., Tahir, M. Y., Nasim, F.-u.-H., Choudhary, M. I., & Khan, K. M. (2008). In vitro cytotoxic, antibacterial, antifungal and urease inhibitory activities of some N 4-substituted isatin-3-thiosemicarbazones. *Journal of Enzyme Inhibition and Medicinal Chemistry*, *23*(6), 848-854.

Pervez, H., Manzoor, N., Yaqub, M., Khan, A., Khan, K. M., Nasim, F.-u.-H., & Choudhary, M. I. (2010). Synthesis and urease inhibitory properties of some new N4-substituted 5-nitroisatin-3-thiosemicarbazones. *Letters in Drug Design & Discovery*, *7*(2), 102-108.

Rizvi, F., Khan, M., Shah, S. Z. A. M., Ali, M., & Siddiqui, H. (2024). New thiosemicarbazone analogues: synthesis, urease inhibition, kinetics and molecular docking studies. *Phosphorus, Sulfur, and Silicon and the Related* Elements, 199(5), 394-405.

Sarıoğlu, A. O., & Soğukömeroğulları, H. G. (2024). Sübstitüe salisiliden Schiff bazı metal komplekslerinin sentezi ve karakterizasyonu. *Gümüşhane Üniversitesi Fen Bilimleri Dergisi*, *14*(4), 1149-1160.

Sevinçli, Z. Ş., Duran, G. N., Özbil, M., & Karalı, N. (2020). Synthesis, molecular modeling and antiviral activity of novel 5-fluoro-1H-indole-2, 3-dione 3-thiosemicarbazones. *Bioorganic Chemistry*, *104*, 104202.

Shakya, B., & Yadav, P. N. (2020). Thiosemicarbazones as potent anticancer agents and their modes of action. *Mini Reviews in Medicinal Chemistry*, *20*(8), 638-661.

Subhashree, G., Haribabu, J., Saranya, S., Yuvaraj, P., Krishnan, D. A., Karvembu, R., & Gayathri, D. (2017). In vitro antioxidant, antiinflammatory and in silico molecular docking studies of thiosemicarbazones. *Journal of Molecular Structure*, *1145*, 160-169.

Tokalı, F. S., Taslimi, P., Usanmaz, H., Karaman, M., & Şendil, K. (2021). Synthesis, characterization, biological activity and molecular docking studies of novel schiff bases derived from thiosemicarbazide: Biochemical and computational approach. *Journal of Molecular Structure*, *1231*, 129666.

Yakan, H. (2020). Preparation, structure elucidation, and antioxidant activity of new bis (thiosemicarbazone) derivatives. *Turkish Journal of Chemistry*, *44*(4), 1085.

Yakan, H., Azam, M., Kansız, S., Muğlu, H., Ergül, M., Taslimi, P., Koçyiğit, Ü. M., Karaman, M., Al-Resayes, S. I., & Min, K. (2023). Isatin/thiosemicarbohydrazone hybrids: Facile synthesis, and their evaluation as anti-proliferatıve agents and metabolıc enzyme inhibitors. *Bulletin of the Chemical Society of Ethiopia*, *37*(5), 1221-1236.

Yakan, H., Muğlu, H., Türkeş, C., Demir, Y., Erdoğan, M., Çavuş, M. S., & Beydemir, Ş. (2023). A novel series of thiosemicarbazone hybrid scaffolds: Design, synthesis, DFT studies, metabolic enzyme inhibition properties, and molecular docking calculations. *Journal of Molecular Structure*, *1280*, 135077.

Zhang, Y.-M., Wang, D.-D., Lin, Q., & Wei, T.-B. (2007). Synthesis and anion recognition properties of thiosemicarbazone based molecular tweezers. *Phosphorus, Sulfur, and Silicon and the Related Elements*, *183*(1), 44-55.

SUPPLEMENTARY MATERIAL

Some new Schiff base derived thiosemicarbazones: Synthesis, spectroscopic characterization, and theoretical studies

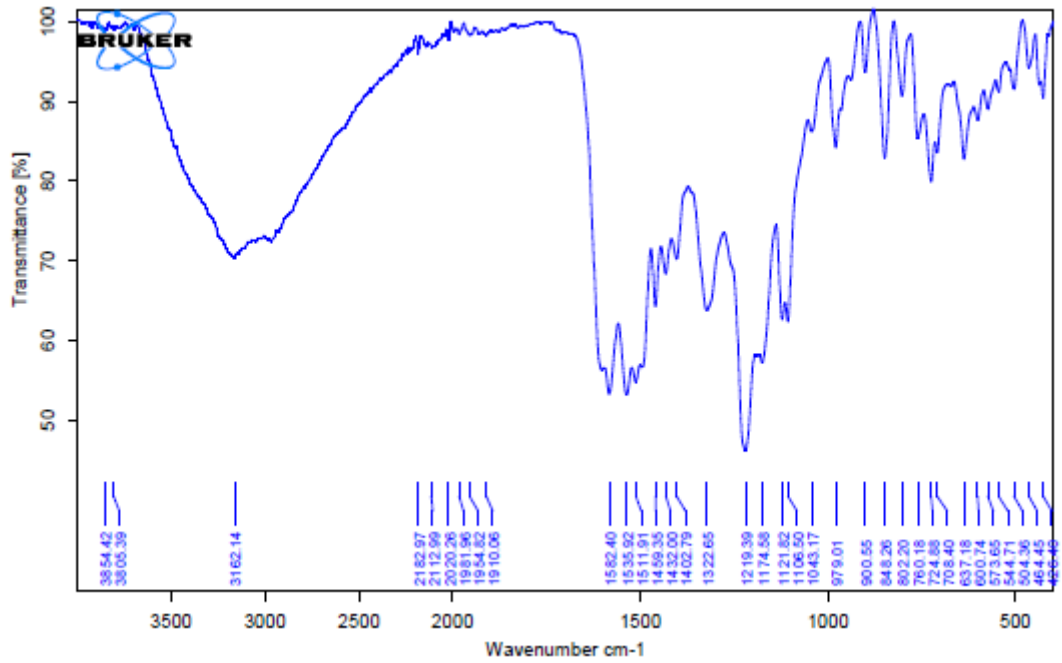

Figure S1. IR spectrum of compound **1**.

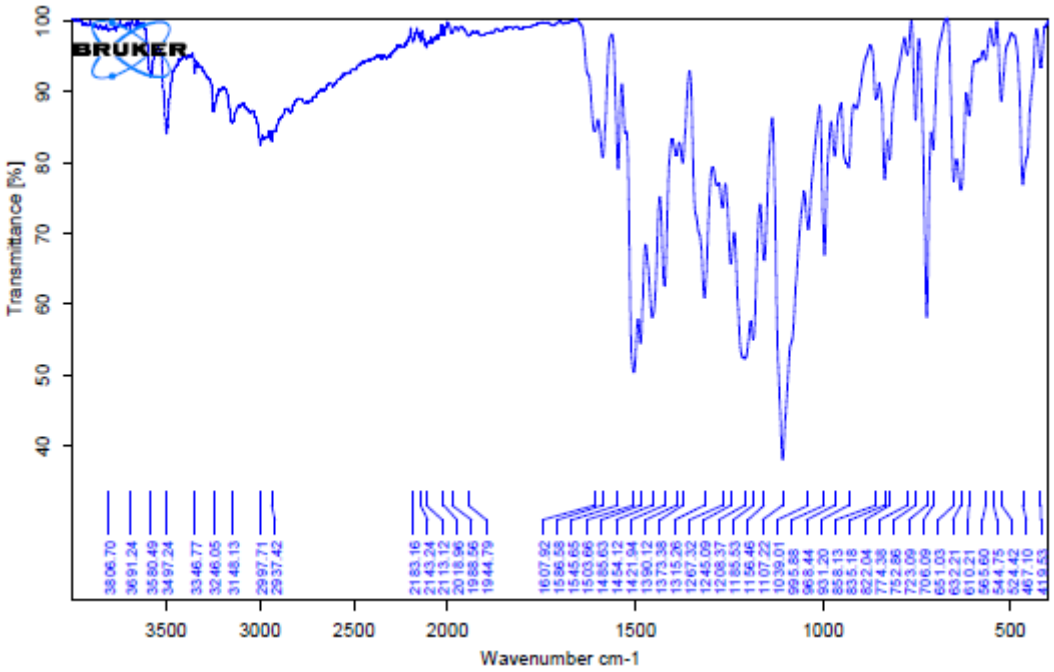

Figure S2. IR spectrum of compound **2**.

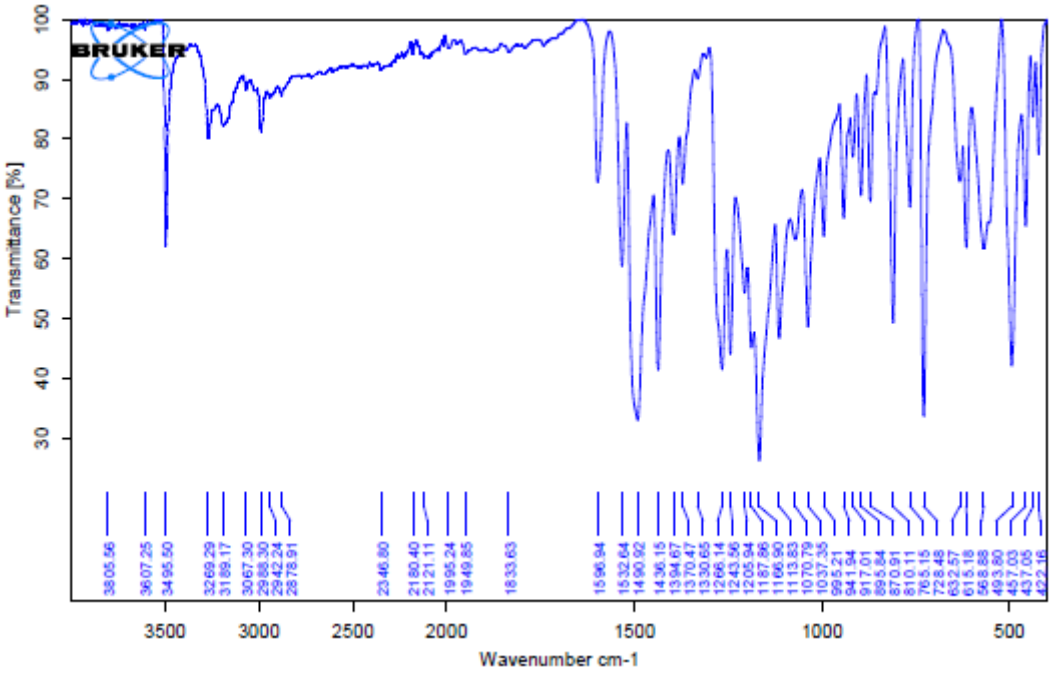

Figure S3. IR spectrum of compound **3**.

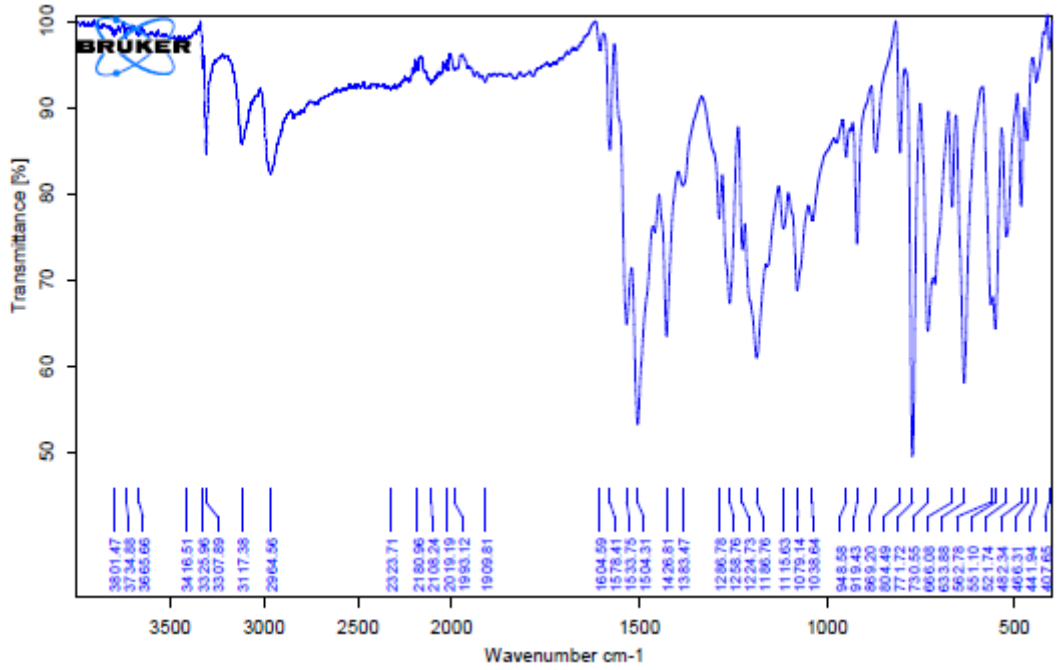

Figure S4. IR spectrum of compound **4**.

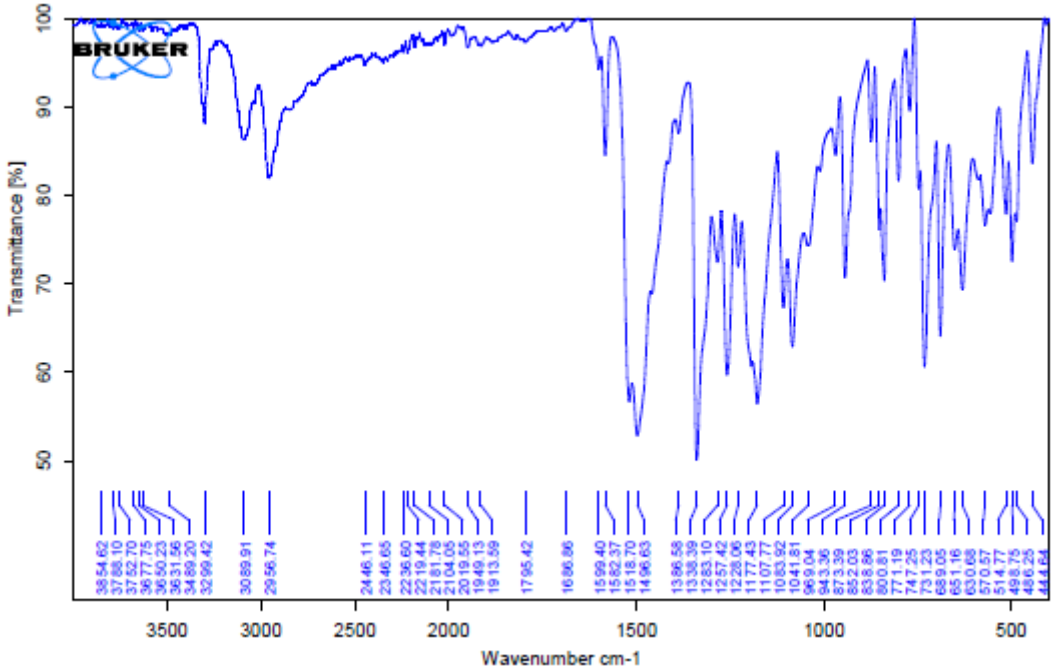

Figure S5. IR spectrum of compound **5**.

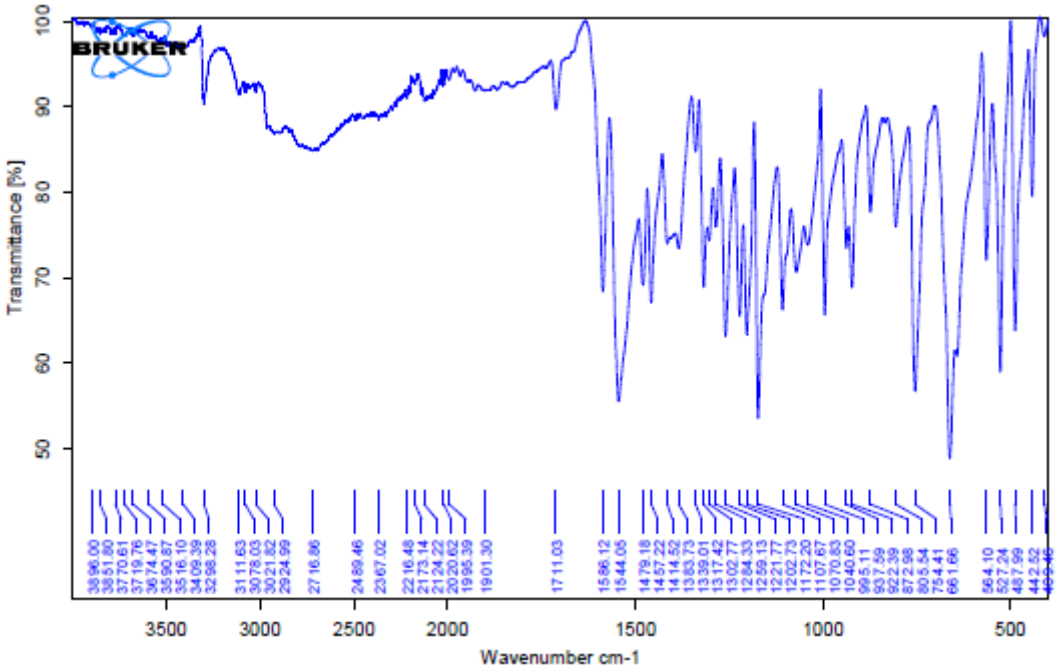

Figure S6. IR spectrum of compound **6**.

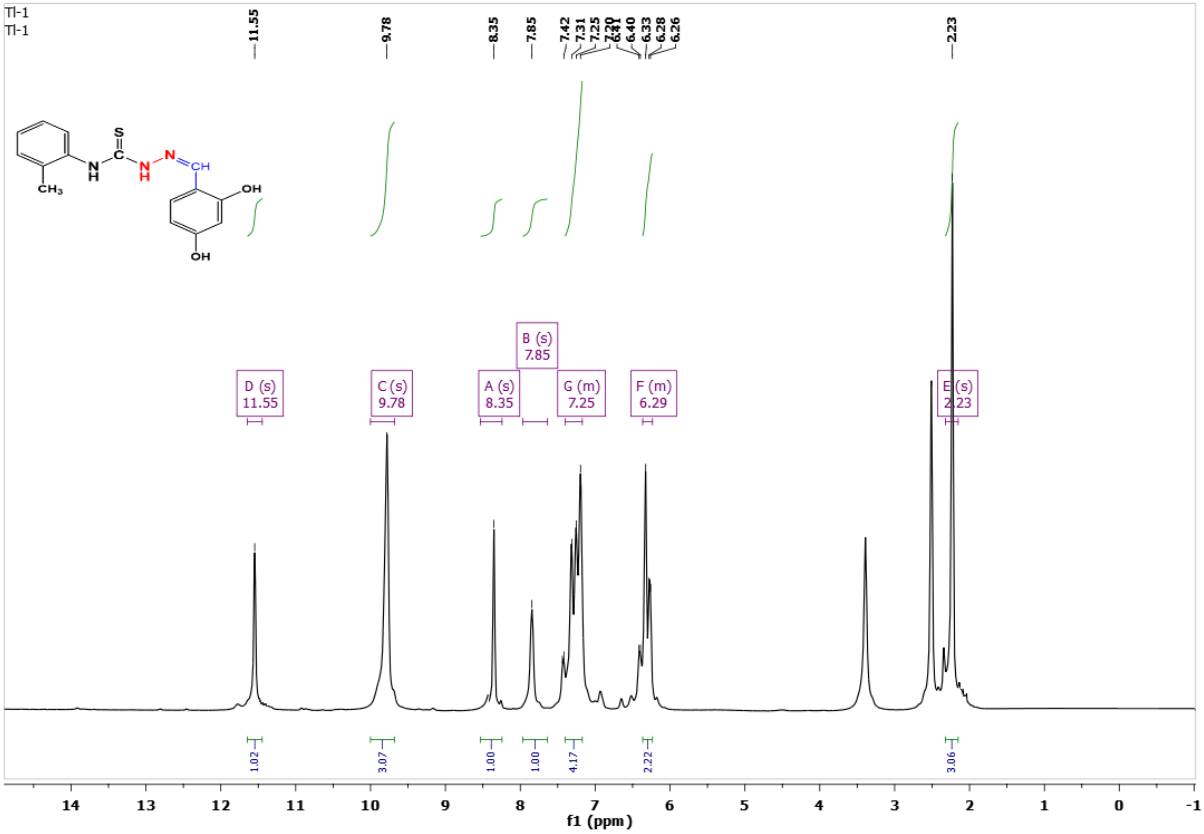

Figure S7. [1]H NMR spectrum of compound **1**.

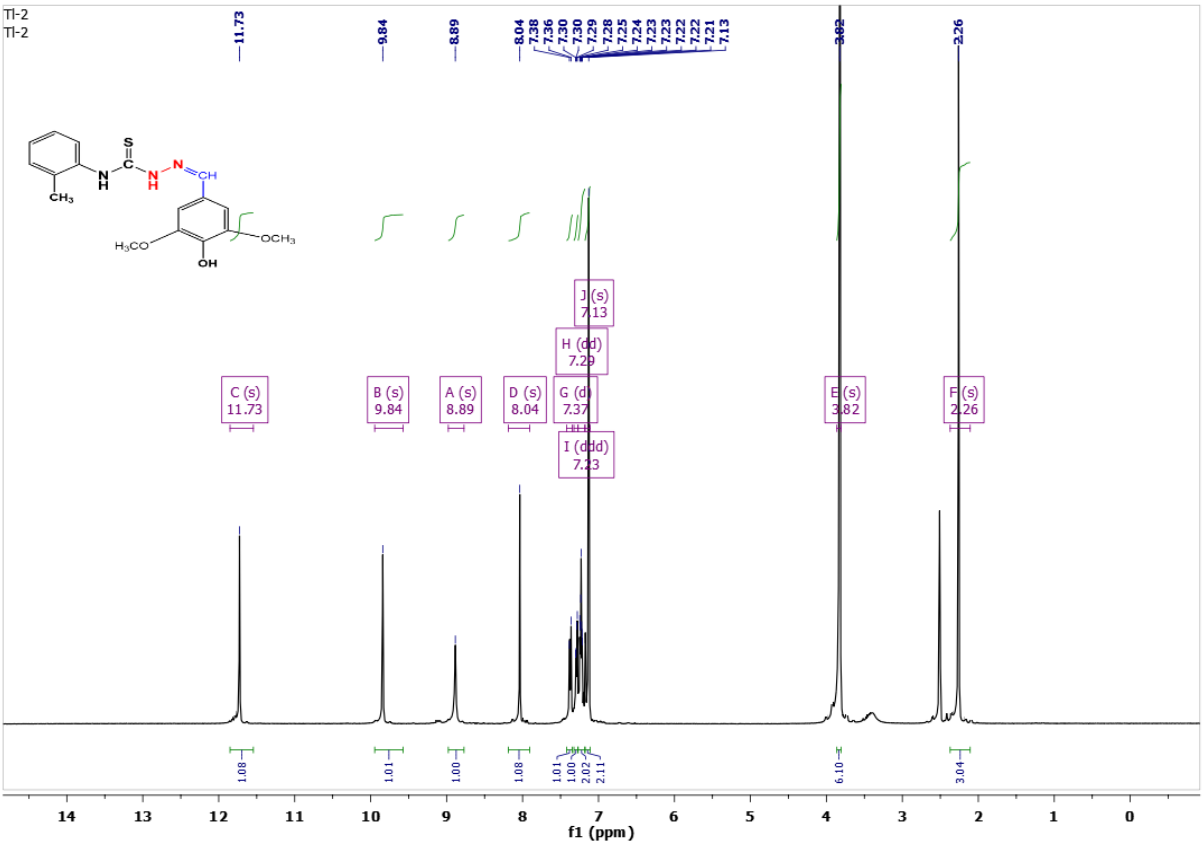

Figure S8. [1]H NMR spectrum of compound **2**.

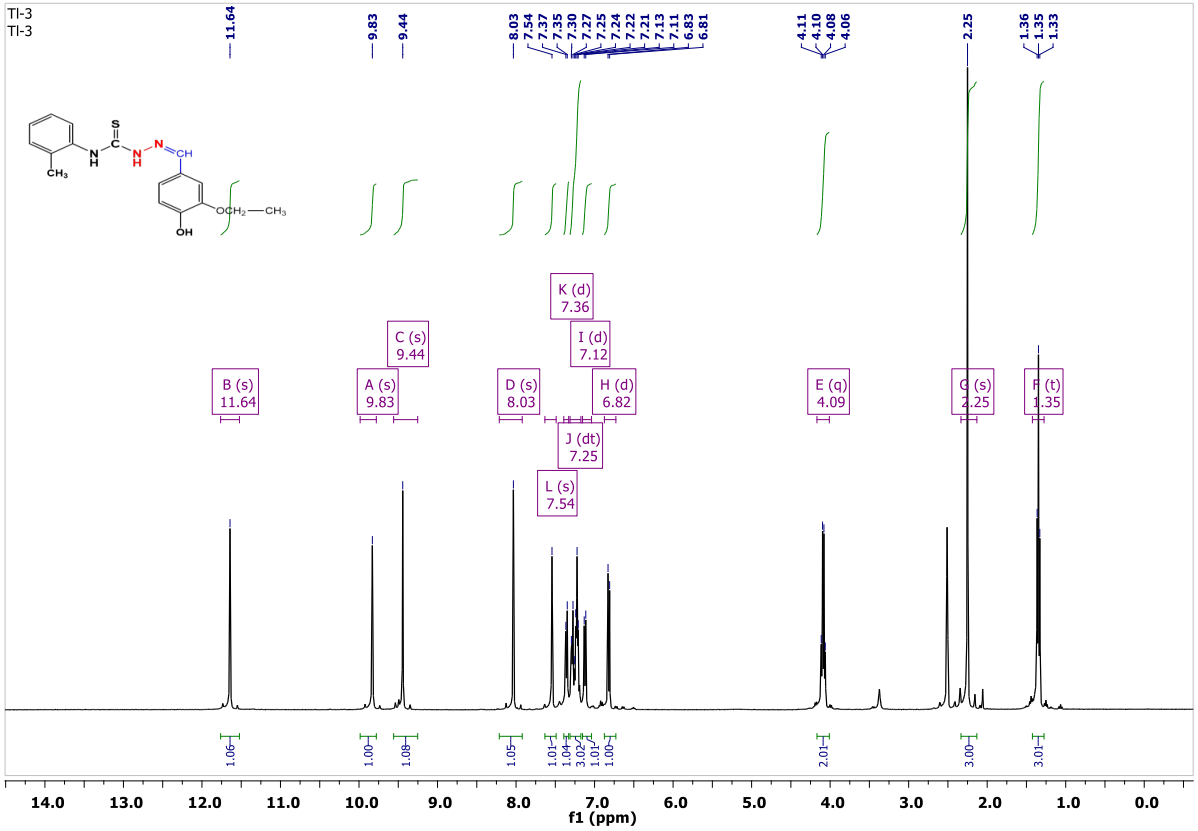

Figure S9. ^{1}H NMR spectrum of compound **3**.

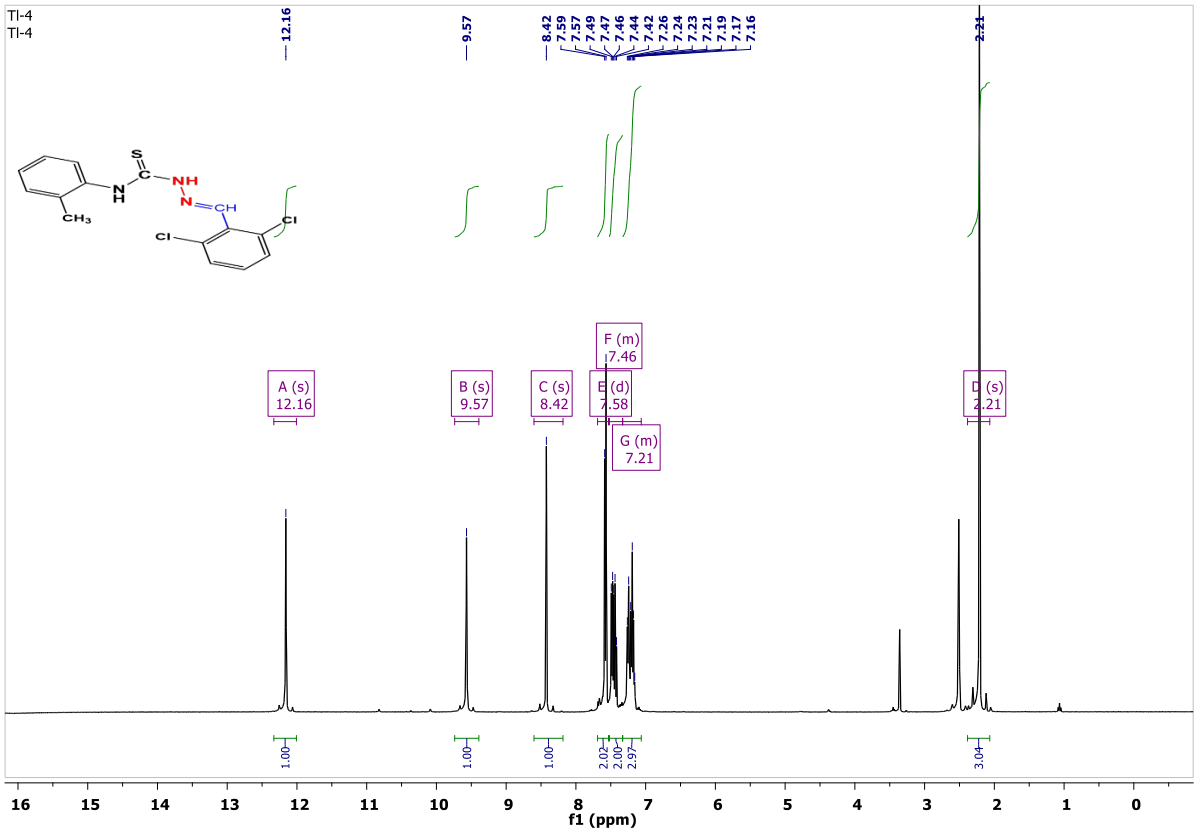

Figure S10. ^{1}H NMR spectrum of compound **4**.

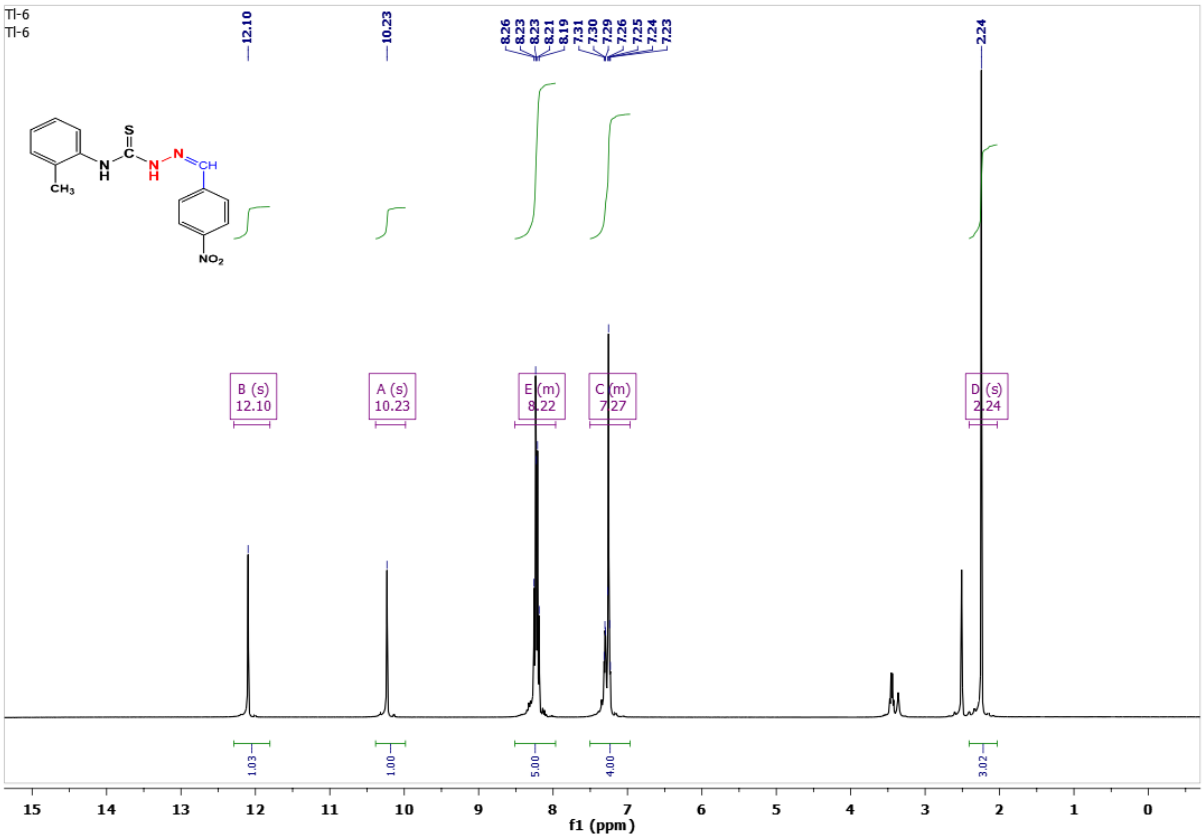

Figure S11. [1]H NMR spectrum of compound **5**.

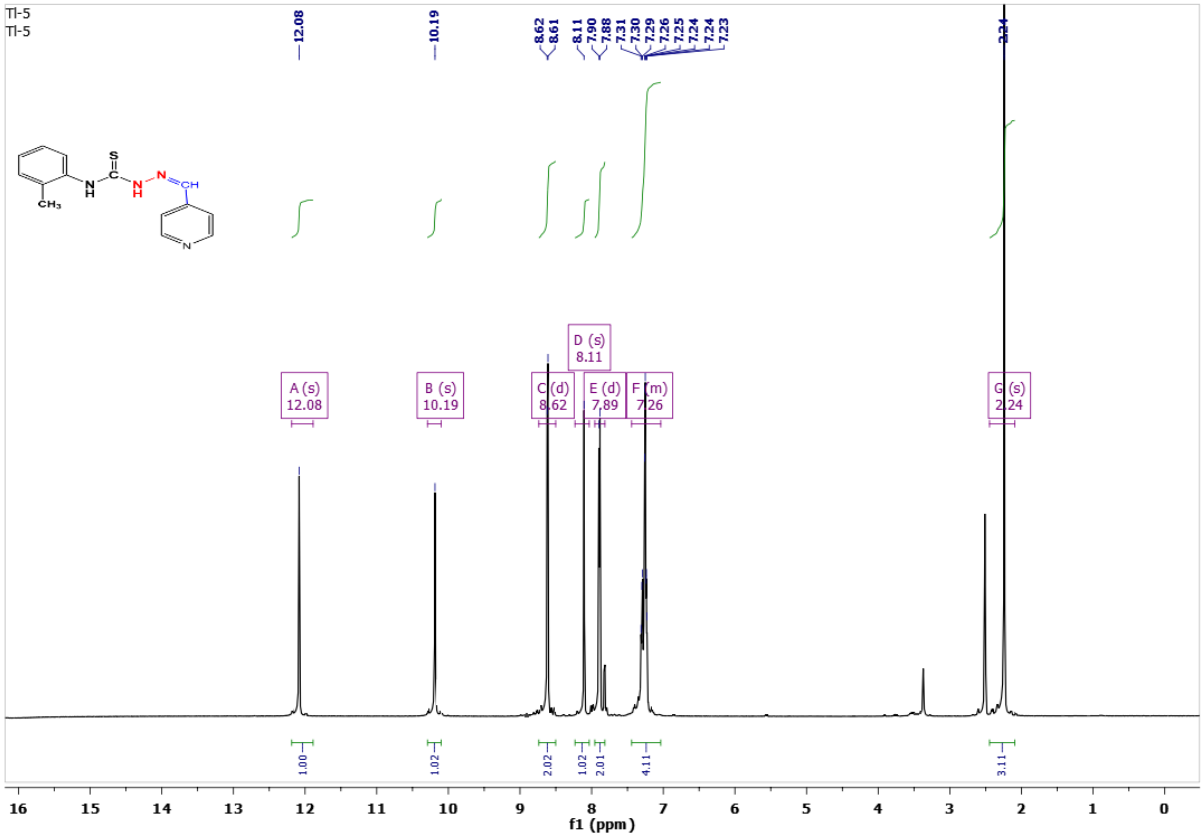

Figure S12. [1]H NMR spectrum of compound **6**.

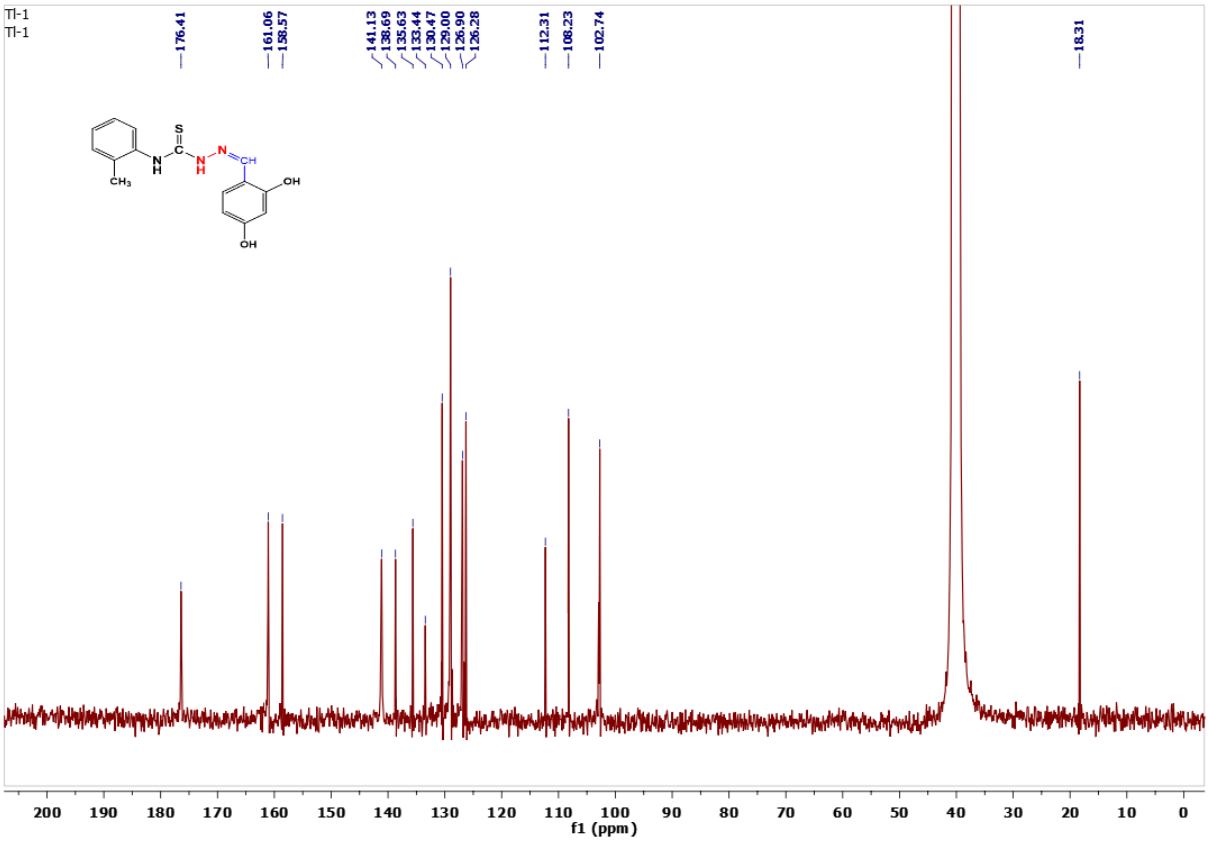

Figure S13. ^{13}C NMR spectrum of compound **1**.

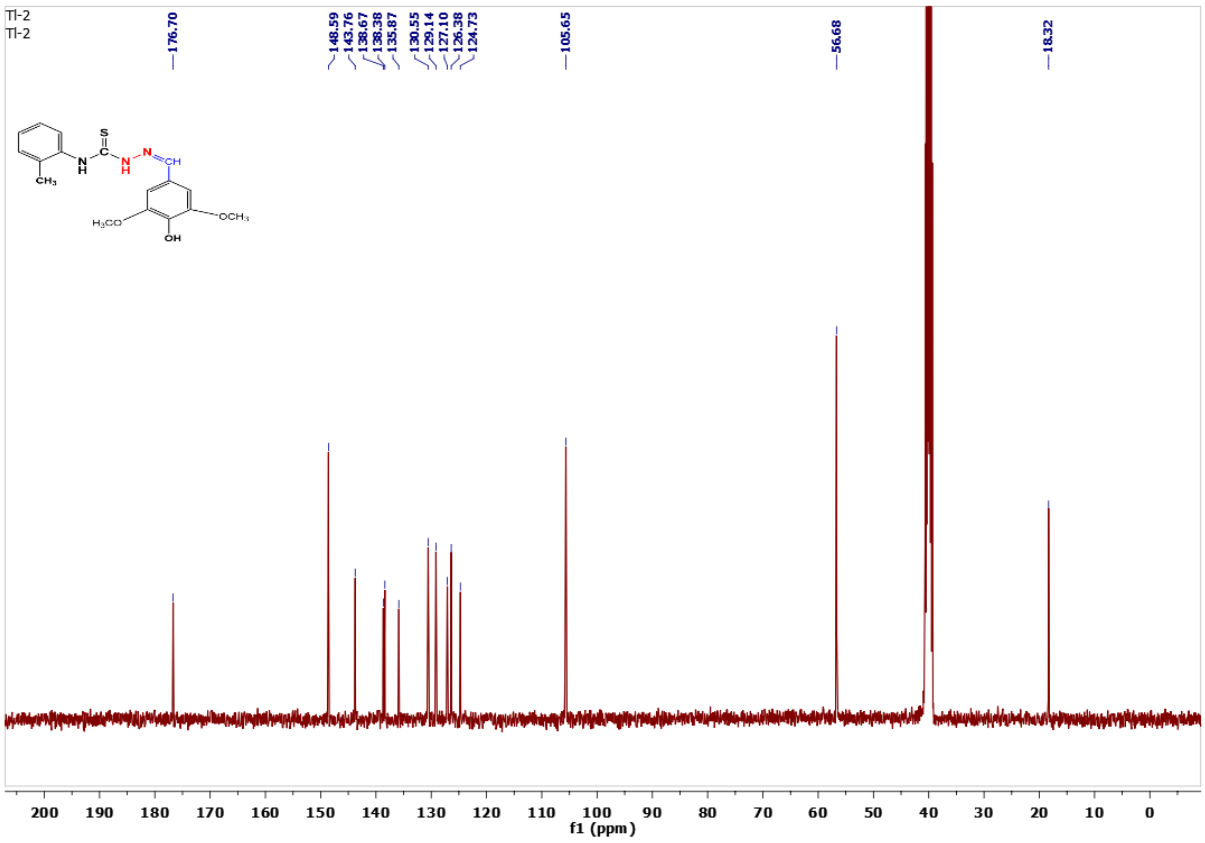

Figure S14. ^{13}C NMR spectrum of compound **2**.

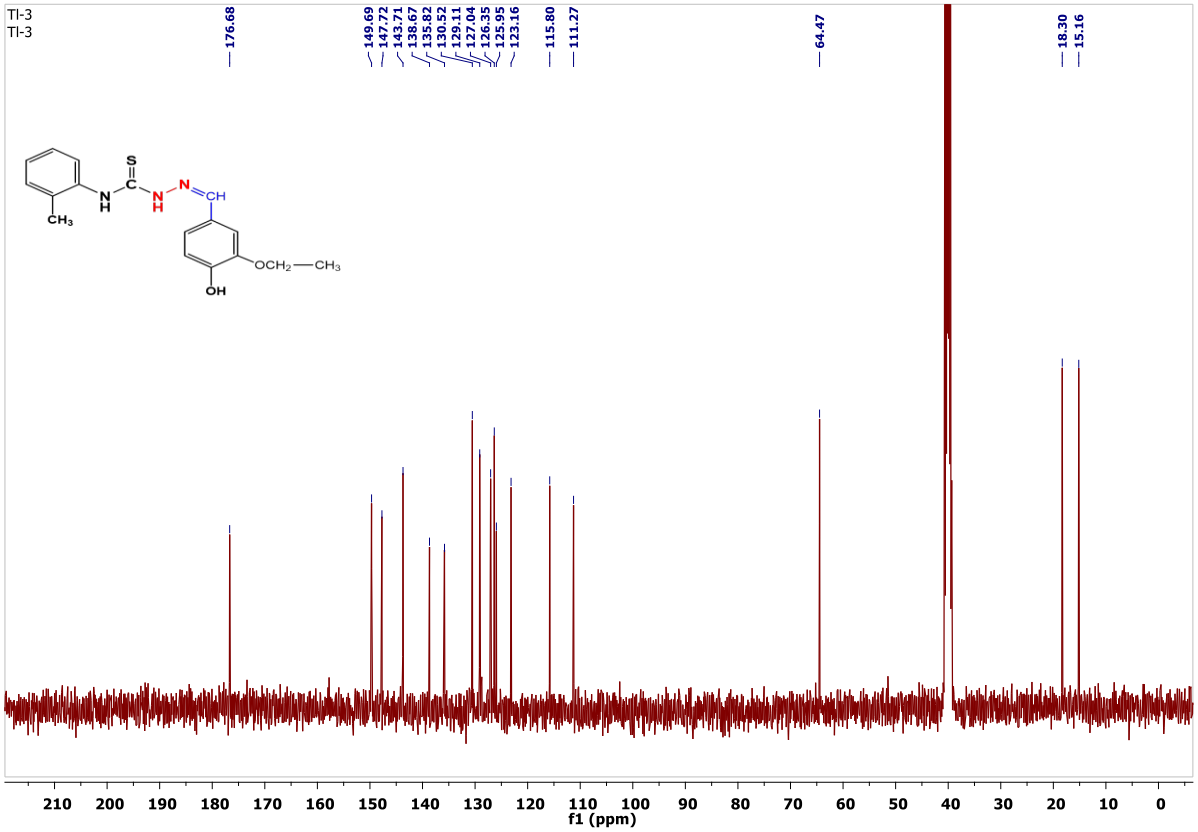

Figure S15. ^{13}C NMR spectrum of compound **3**.

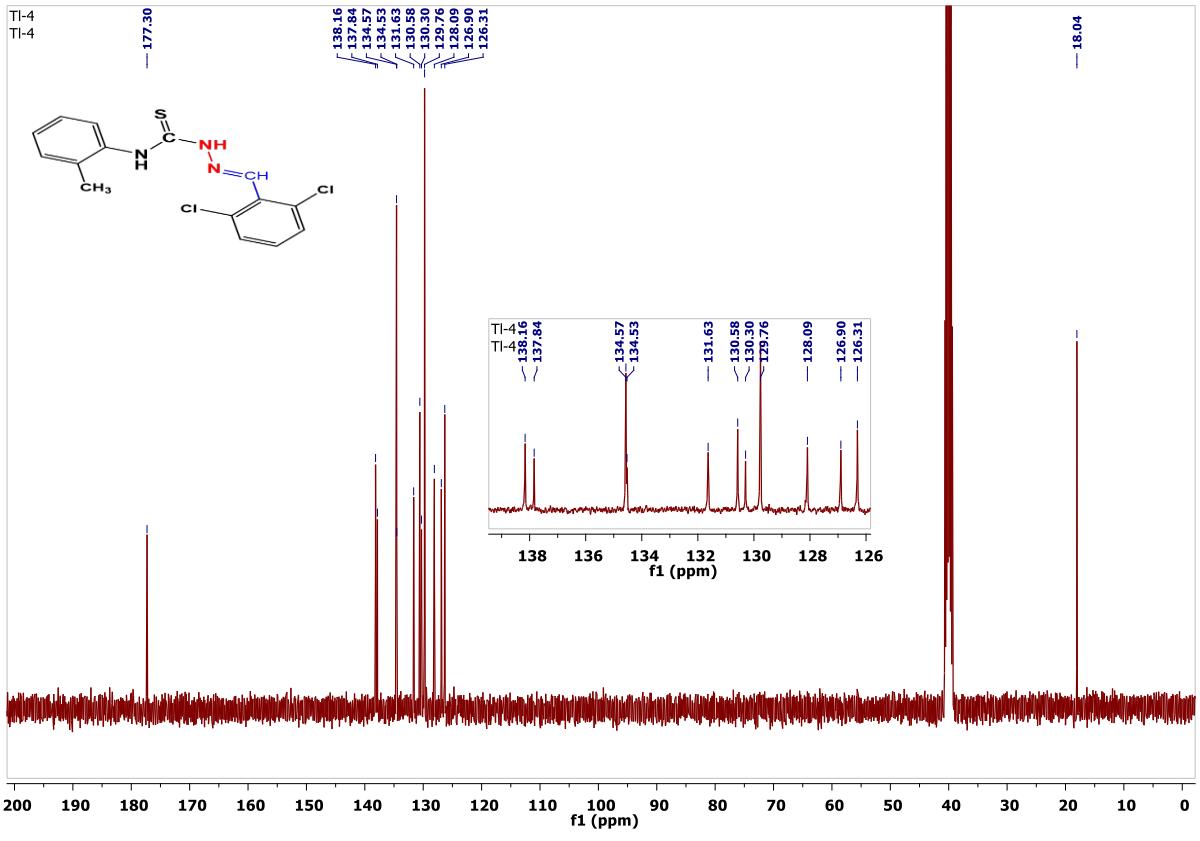

Figure S16. ^{13}C NMR spectrum of compound **4**.

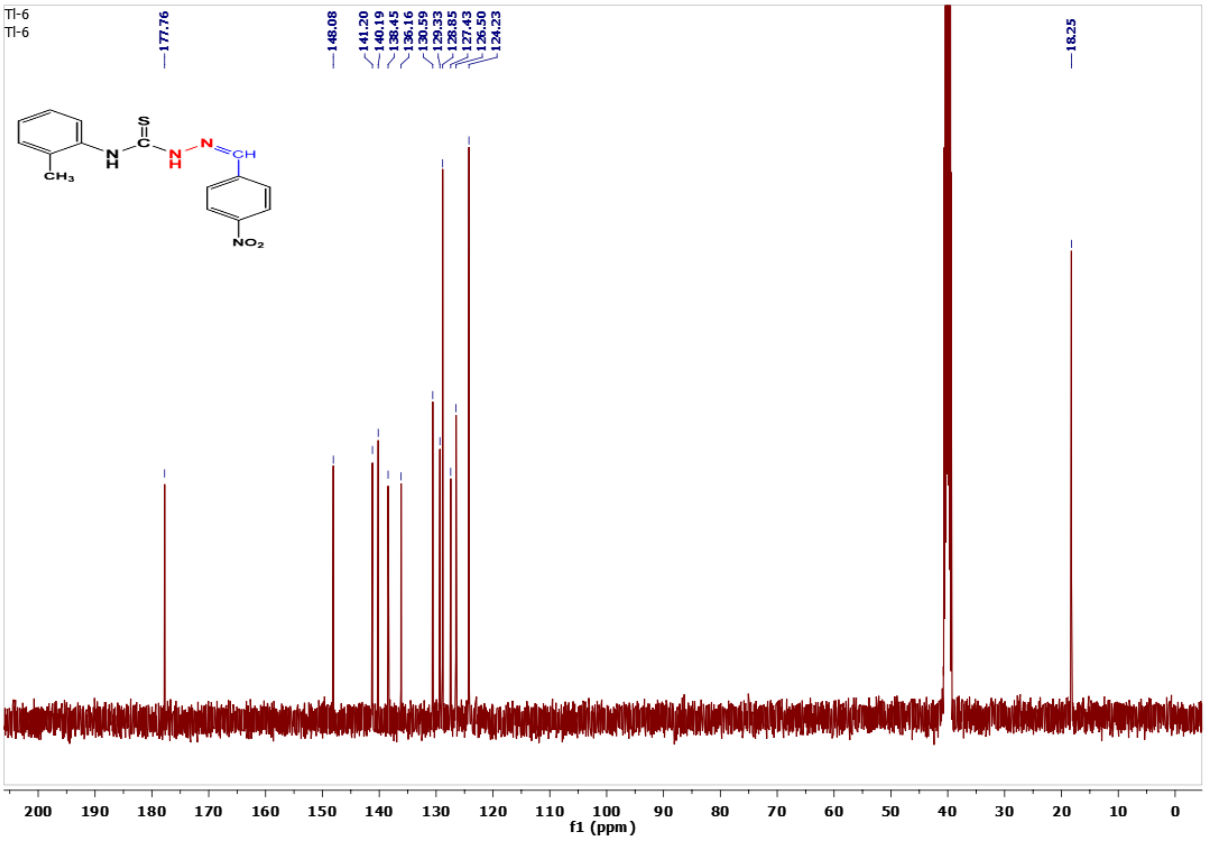

Figure S17. ^{13}C NMR spectrum of compound **5**.

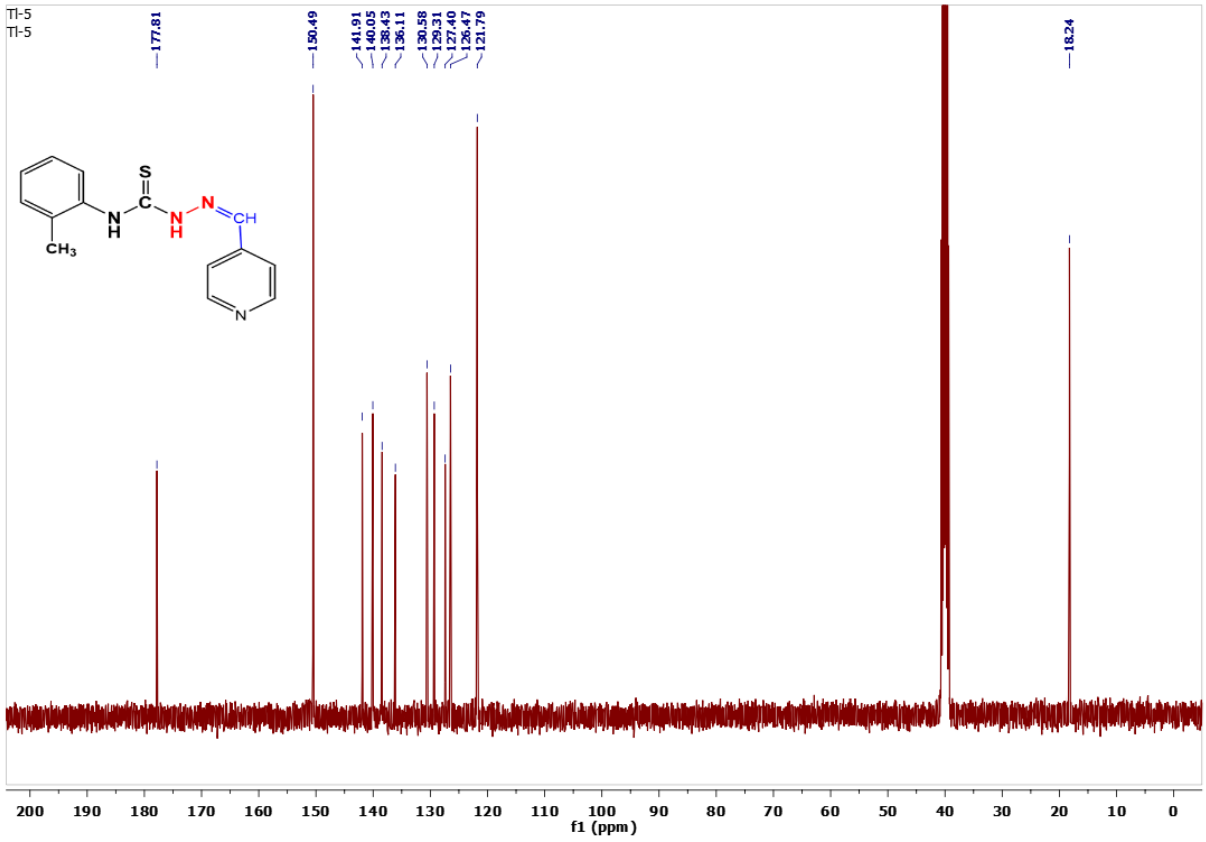

Figure S18. ^{13}C NMR spectrum of compound **6**.